crystals

MDPI

Article

Interactions on the Interface between Two Liquid Crystal Materials

Rok Geršak † and Simon Čopar *

Faculty of Mathematics and Physics, University of Ljubljana, 1000 Ljubljana, Slovenia; rok.gersak@gmail.com
* Correspondence: simon.copar@fmf.uni-lj.si
† Current address: GEN-I d.o.o., Vrbina 17, 8270 Krško, Slovenia.

Received: 26 April 2020; Accepted: 11 May 2020; Published: 14 May 2020

Abstract: In liquid crystal applications, boundary conditions are essential to ensuring suitable bulk molecular orientation and a deterministic response to external fields. Be it confinement to a droplet or a shell, a glass plate, or an interface with air or another liquid, proper surface alignment must be ensured—mechanically by rubbing, by chemical treatment that adds a layer of aligning molecules, by using photoalignment or even by leaving the surface untreated, using the intrinsic properties of the substrate itself. The anchoring can be classified as unidirectional (perpendicular homeotropic, or at oblique angles), or degenerate (planar or pre-tilted). However, if both substances at the interface are anisotropic, more diverse behaviour is expected. Here, we present a numerical simulation of a nematic droplet in a nematic host, and investigate behaviour of the director field and defects at the interface for different interfacial couplings. Finally, we compare the simulations to experimental images of discotic droplets in a calamitic nematic host.

Keywords: surface anchoring; anisotropic interface; Landau-de Gennes

1. Introduction

Liquid crystals are most known for their use in displays, but in recent years they are also emerging as promising materials in photonics and lasing [1]. As liquid crystals have a key role in studies of shape-switching and self-assembling materials, several liquid crystal systems, among others liquid crystal colloids, liquid crystal suspensions and emulsions, have been intensively studied [2–5]. However, systems with two anisotropic materials in contact remain a harder challenge and so both experimental and theoretical studies of such mixtures are rare. A few such systems emerged in active lyotropic-thermotropic mixtures, where the activity induced motion of defects in the thermotropic phase [6,7]. Interactions among the constituent parts of two anisotropic materials are, in contrast to the well studied contact region between a liquid crystal and an isotropic material, far more diverse at a contact region between two liquid crystals.

In confined liquid crystals, orientation of the molecules at the surface is one of the contributions that affects equilibrium orientation within the liquid crystal. This contribution is especially important in more complex geometries, like in liquid crystal droplets, as prescribing orientation at surfaces may create a variety of topological defects. There are plenty of studies of relations between the preferred orientation at the surface and the corresponding structures inside or around droplets in nematic and cholesteric mixtures [4,8–14].

When a nematic droplet is in contact with an isotropic material, interaction between the nematic and its surface determines the type of a surface anchoring that is, preferred orientation of molecules at the interface. In a case of two anisotropic materials in contact, the situation is little different, since the materials can also interact anisotropically with each other. Three coupling models are required to

describe interactions between the three orientational parameters at the interface: the surface normal and directors of both materials.

In this paper, we use numerical Landau-de Gennes modeling of a two-phase system of two nematics, to explore various combinations of anchorings that correspond to different interactions between liquid crystalline materials at the interface. We use the geometry of a droplet to demonstrate what orientational textures and topological defects arise in different configurations. Finally, we compare our results with an experiment realization in a discotic-calamitic liquid crystal system.

2. Materials and Methods

A nematic two-phase system is modeled with a Landau-de Gennes free energy approach, where free energy is a weighted sum of bulk and surface contributions. All contributions are constructed with the tensorial order parameter Q_{ij}, which in contrast to the director also characterizes the defect regions. For thermotropic liquid crystals bulk contributions consist of the Landau expansion around the nematic-isotropic transition, and of the elastic energy [15,16]. In our model the latter was approximated with one elastic constant. The surface contribution is in general composed of three terms—coupling of each nematic material to the surface, and direct coupling of both directors to each other, each with its own coupling constant. Free energy thus consists of [17–19]:

$$\begin{aligned} F = & \sum_{n=1,2} \iiint \left\{ \frac{1}{2} A Q_{ij}^n Q_{ji}^n + \frac{1}{3} B Q_{ij}^n Q_{jk}^n Q_{ki}^n + \frac{1}{4} C \left(Q_{ij}^n Q_{ji}^n \right)^2 \right\} \rho \mathrm{d}V \\ & + \sum_{n=1,2} \iiint \left\{ \frac{1}{2} L_1 \frac{\partial Q_{ij}^n}{\partial x_k} \frac{\partial Q_{ij}^n}{\partial x_k} + 2 L_1 q_0 \epsilon_{ikl} Q_{ij}^n \frac{\partial Q_{lj}^n}{\partial x_k} \right\} \rho \mathrm{d}V \\ & + \iiint \left\{ f_{SA} \left(\nabla\rho / |\nabla\rho|, Q_{ij}^1 \right) + f_{SA} \left(\nabla\rho / |\nabla\rho|, Q_{ij}^2 \right) + f_{NA} \left(Q_{ij}^1, Q_{ij}^2 \right) \right\} |\nabla\rho| \mathrm{d}V, \end{aligned} \tag{1}$$

where the first term is the Landau expansion with material parameters A, B and C, the second term with the elastic constant L_1 accounts for elastic distortions in both the non-chiral and chiral nematics, where uniform helical axis is characterized by the inverse pitch q_0, and the third term evaluates the contribution of the three anchorings. The Q-tensors Q_{ij}^1 and Q_{ij}^2 respectively refer to the tensorial order parameter in the outer and the inner nematic phase. In addition to this, ρ represents the phase field that is 1 in the first material, 0 in the second, and the gradient $\nabla\rho/|\nabla\rho|$ is largest at the transition between both materials [20,21]. The normalized gradient $\nabla\rho/|\nabla\rho|$ determines the normal to the interface, which plays a role in the anchoring energy [20,22].

Each of the three anchorings describes interaction between the two of the three directions in the anisotropic two-phase system—both directors and the surface normal. We consider two options—using the Nobili-Durand model [19,23], if directions tend to align parallel to each other (homeotropic anchoring), and the Fournier-Galatola model, if the directions prefer to be perpendicular (planar anchoring) [23]. Both models were originally constructed for the interaction between the surface normal and the director. We adapt these models for nematic-nematic anchoring. One material (e.g., the inner nematic phase) plays the role of the director and the other (e.g., the outside nematic phase) plays the role of the surface normal. With combinations of these three anchoring types, we can describe a variety of potential experimental situations. For example, the nematic-nematic coupling is, in the absence of additional chemical interactions, expected to be planar for a discotic-calamitic interface, if the rods sterically prefer to lie flat on the disks. The nematic-to-surface normal coupling can be affected by the same parameters as in the nematic-isotropic interfaces, such as entropic effects, hydrophilic-hydrophobic interactions, and effects of surfactants. The strengths of the couplings will in principle be unique for each pair of materials, and will in general vary with temperature.

The equilibrium configuration of the director field in the nematic systems is obtained with the minimization of the free energy [18]. Whether the minimized configuration is really an equilibrium and not meta stable mainly depends on the initial configuration of the director field. We minimize

the free energy F (Equation (1)) numerically on an equidistant cubic finite difference grid, where in each grid point both tensorial order parameters that account for the two nematic materials are the active variables. The phase field ρ was not an active variable, but was fixed to specify the shape of the interface, which in our case was one or two droplets. If needed, hydrodynamic equations can be added for a fully dynamic two-phase model [20,21]. This is relevant for shape-control applications, where variations in surface energy or active flow can affect static or dynamic shape modulation [24–26].

In simulations material parameters of a nematic liquid crystal 5CB are used: $A = -0.172 \times 10^6\,\mathrm{J/m^3}$, $B = -2.12 \times 10^6\,\mathrm{J/m^3}$, $C = 1.73 \times 10^6\,\mathrm{J/m^3}$, and the distance between the grid points is set to $\Delta x = 9$ nm [12,18]. The material parameters are chosen as a benchmark; for case-specific simulations, they should be tuned to the utilized materials. In order to distinguish between the three anchoring constants that exist in anisotropic two-phase systems, we mark the nematic in the droplet with index 1, the outside nematic with index 2, and the surface with index p. Furthermore, we mark the homeotropic type of anchoring with *hom* and the planar degenerate anchoring with *deg*. If not stated differently, elastic constant has value $L_1 = 4 \times 10^{-11}$ N, and the boundary condition of the outside nematic is a flat planar cell. Anchoring constants in the test cases with a single droplet are strong, $W = 10^{-3}\,\mathrm{J/m^2}$, allowing us to observe observe the behaviour in the extreme case. For weaker anchoring, we expect similar structures, but with less abrupt director transitions and defects closer to the surface.

3. Results

An equilibrium state in nematic droplets depends on the type of the surface anchoring, droplet size, and in the case of the chiral nematic also on the chirality parameter N, measuring the number of π-turns per droplet diameter [3,13]. In numerical simulations that are shown and discussed in below subsections, main focus was on different combinations of anchorings between the nematic droplet and the outside nematic, however, the elastic constant L_1, the chirality parameter N and the number of droplets were also varied for specific tests.

The three couplings that tend to describe interactions between the two nematic materials are either of the planar degenerate or of the homeotropic type. As we are exploring general behaviour of different couplings, we assume all couplings to have the same coupling constants W, and we limit ourselves to couplings that do not lead to frustration at the border. Such frustrations would lead to decrease in nematic order near the surface, which would make the behaviour similar to a contact with an isotropic material with a low preferred surface order.

3.1. Nematic Droplet

We studied different coupling combinations on a droplet suspended in the outside medium with uniform external far-field. In the combination with all anchorings of the homeotropic type, one expects the outside to behave as a nematic around a colloidal particle with homeotropic anchoring, and the inside as a homeotropic nematic droplet [11]. As seen from the Figure 1a, this behaviour is indeed observed. Outside the droplet, a Saturn ring defect is formed, while on the inside, we find a central point defect, with point defect expressed as a small ring defect, as is seen in most simulations. In practice the exact form of the point defect depends on elastic constants, temperature, size of the droplet, and flexoelectricity [27–29].

A similar example is shown in Figure 1b, with outside material preferring homeotropic alignment to the surface, and the inside material favoring planar anchoring. In this situation, there is a discontinuity of director at the surface. The outside still forms a Saturn ring. The inside resembles a planar droplet with bipolar director structure [3]. However, instead of two surface point defects (boojums), disclination loop segments span across the surface.

Homeotropic anchoring is very restrictive, and effectively isolates the outside from the inside. In such cases, we expect structures very similar to structures in droplets and around colloidal particles, such as the two shown in Figure 1. A more interesting combination is produced if all three anchorings are of planar degenerate type. Such anchoring leaves the director on both sides one degree of freedom,

constrained to be perpendicular to each other across the interface. Due to the spherical geometry, droplets with the planar degenerate surface anchoring have defects on the surface, either two defects with winding number $+1$, or four defects with winding number $+1/2$. These must be endpoints of disclination lines that exist in the bulk, similar to the inside structure of the case in Figure 1b. The defect is forced to penetrate the surface, and continue on the other side, as observed in Figure 2. We find a closed defect loop, going through the bulk of the droplet, and sticking out to the outside material on opposite sides in the direction of rubbing. As the materials on the outside and the inside are different, the shape and size of the defect loop can vary according to the ratio of elastic constants. We simulated the same structure for a larger value of the outside elastic constant L_2, more specifically, $L_2 = 8 \times 10^{-11}$ N, twice as large as the elastic constant inside. The results are shown in Figure 2. As a consequence of a more rigid nematic, defects outside of the droplet are thicker and tend to shorten. The phase parameters, A, B and C, are in this case kept constant, but the effect of varying them would be similar if they were varied as well, as the main parameter that drives the transformation is the disclination line tension, which depends on both the elastic constants and the nematic correlation length, $T = \frac{K\pi}{2} \ln \frac{D}{\xi}$, D being a characteristic physical size of the system [15].

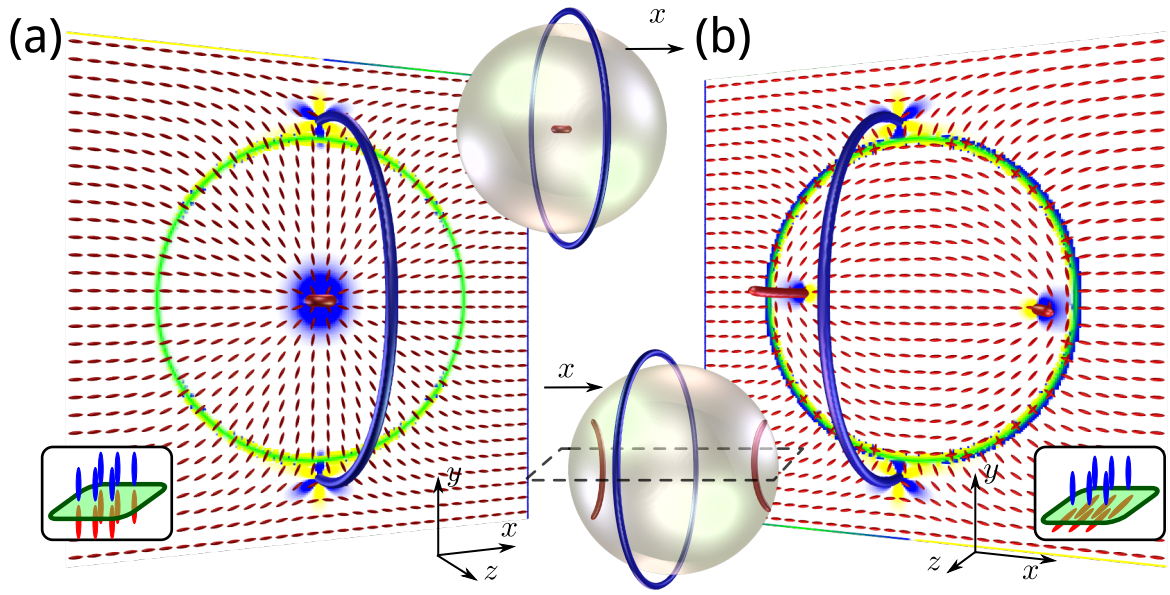

Figure 1. Nematic structures in a droplet in homogeneous director field along the x direction, with two different types of anchoring. (**a**) For coupling constants W_{1S}^{hom}, W_{2S}^{hom}, W_{12}^{hom}, a Saturn ring is formed outside the droplet, and radial director with a point defect forms in the middle. (**b**) For coupling constants W_{1S}^{deg}, W_{2S}^{hom}, W_{12}^{deg}, the outside is similar, but the inside behaves as a planar nematic droplet with two defect segments on the opposite sides. Defects are isosurfaces at $S = 0.48$, blue for the outside and red for the inside defects. The colours depict the splay-bend parameter [30], highlighting the features of the director—blue shows high splay and yellow high bend deformation. Insets depict the type of anchoring: green represents the interface, red and blue represent the inside and outside director, respectively.

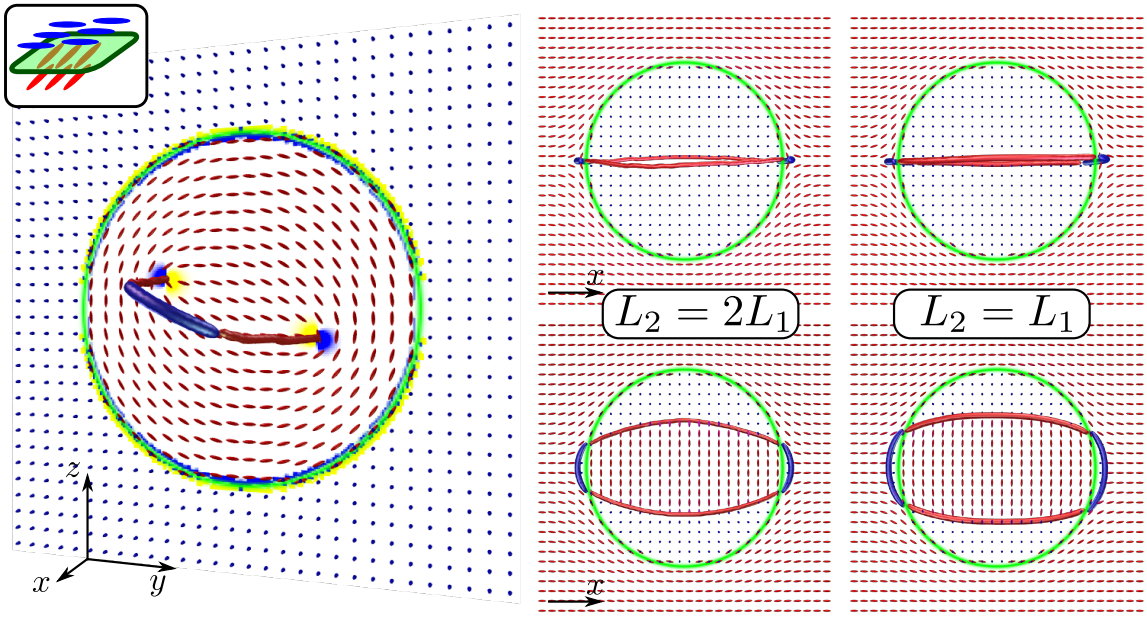

Figure 2. A nematic structure obtained when all three coupling constants are planar degenerate (directors perpendicular to the surface normal and to each other). A defect ring is formed that penetrates the surface of the droplet on the opposite poles, even though the director rotates by 90° on the transition from the inside to the outside. If elastic constants are different outside and inside, the shape of the disclination ring changes. The main panel depicts the cross section perpendicular to the far field, while the small panels show the cross sections perpendicular and parallel to the plane of the defect ring. Main panel and left column represent $L_2 = 2L_1$, with outer structure being stiffer, and the right column has equal constants in both materials.

3.2. Cholesteric Droplet

We also considered different couplings for a two-phase system with a cholesteric droplet in a nematic host. The focus was on finding the general behaviour of how the structures in cholesteric droplets change in the presence of the nematic-nematic interaction. Chirality is measured by N, the number of half-twists per droplet diameter.

First, consider the case with homeotropic inner anchoring, planar outside anchoring, and compatible planar nematic-nematic anchoring. Figure 3a shows a regular nematic droplet, which shows boojums at the poles on the outside and a central point defect inside [3]. With introduction of mild chirality $N = 1.5$, the point defect offsets from the center (Figure 3d), creating a familiar twisted chiral soliton structure inside [14,31,32]. However, the outside and inside director structures are not aligned to a common symmetry axis. The coupling between the two structures is very weak, because the outer part of the internal structure is almost rotationally symmetric. With weaker anchoring, the interaction would become more significant. We also tested higher chiralities and different combinations of anchorings. For example, Figure 3b shows a structure with homeotropic anchoring outside and planar inside, with matching nematic-nematic coupling, at $N = 6$. In this case, the internal nematic resembles the onion-like diametric spherical structure [12], which has defects and areas of large deformation close enough to the surface, that it aligns with the Saturn ring outside, although an additional rotational degree of freedom remains around the far-field direction. Similarly, if all anchorings are homeotropic (Figure 3c), which at $N = 3$ internal chirality allows an equatorial Saturn ring. The disclination line in this case has a twist cross section.

As with the nematic, the cholesteric case yields the most interesting structures when all couplings are planar, creating two mutually perpendicular planar director fields at both sides of the interface. Figure 3e shows that we obtain a structure consisting of two boojums with winding number $+1$ on the

surface, not diametrally, but closer together. Due to chirality, set in this case at $N = 3$, internal twist is induced across the droplet, as seen in the cross section. The boojums are expected to continuously move together from diametral structure in the absence of chirality, to very close for higher chirality, as seen in planar droplets in isotropic host liquid [12,33]. However, the perpendicularity on the surface creates an interesting boundary condition in the outside nematic, which is in a different, achiral homogeneous far field. This is thus the coupling that is most interesting to pursue further experimentally.

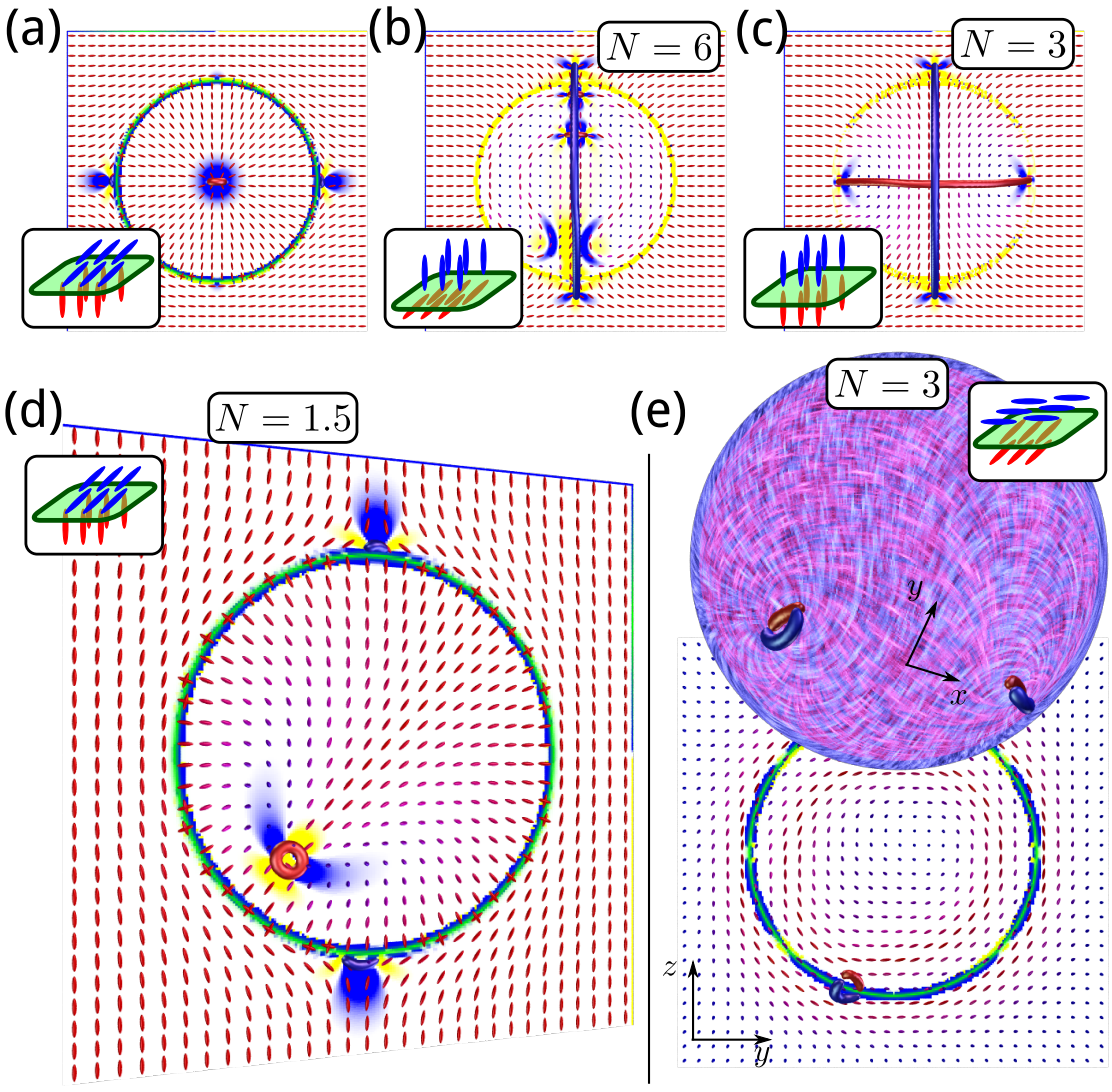

Figure 3. Different combinations of chirality and anchoring. (**a**) Achiral case: a combination of W_{1S}^{hom}, W_{2S}^{deg}, W_{12}^{deg} results in a radial structure on the inside and two boojums, behaving as a colloidal particle with planar degenerate anchoring, on the outside. (**b**,**c**) For cholesteric inner phase and nematic outer phase, we also see combinations of well known outside and inside behaviour (shown for two chiralities and two anchoring combinations). We obtain the (**b**) onion structure and (**c**) the equatorial Saturn ring with chiral escape inside. (**d**) Homeotropic inner anchoring is very weakly coupled to the structure outside, allowing rotational degeneracy (shown is a single off-center point cholesteric defect structure at an arbitrary angle to the outside director). (**e**) Inner cholesteric, with outside and inside perpendicular to each other and the surface normal, results in dual, mutually perpendicular inside and outside surface directors with two non-diametral boojums. The red and blue streaks show the inner and outer director, respectively.

3.3. Droplet Dimer

Topological defects tend to induce forces between droplets or solid particles in nematic two-phase systems. In the case of homeotropic anchoring, single long disclination loops may entangle multiple particles together [2,5,34–36]. We simulated a system of two droplets in close proximity with homeotropic anchoring on the outside, planar anchoring on the inside, and planar nematic-nematic anchoring. This anchoring condition is chosen to correspond to preliminary experiments conducted by the researches of the Jožef Stefan Institute with a discotic-calamitic mixture in a twisted nematic cell. A 11 %wt. mixture of a discotic compound (19b substance described in Reference [37]) and a calamitic compound (eutectic E18 mixture), phase separates into discotic-dominated droplets suspended in a calamitic-dominated host liquid. Our simulation was set up to approximate the entangled dimer of discotic droplets, as shown in Figure 4). In agreement with the experiment, we employ 90° twisted boundary condition of the planar cell, with mid-plane director perpendicular to the separation between the particles.

Experimental transmission image of this experiment, done between crossed polarizers with a red full-wave plate reveals that at the specified mass fraction of the discotic material, droplets form. Clusters of two or more droplets can be found, such as the interacting dimer seen in Figure 4c. Disclination lines assume an entangled conformation, known from previous experiments in a twisted nematic cell with homeotropic anchoring [38], implying that the anchoring on the outside nematic is homeotropic. For this boundary condition, different variants of entanglement, such as figure-eight, figure-omega and figure-theta [5], are expected. The micrograph indicates that the disclination line is not seen in the bulk material, instead lying directly at the interface. This is expected for weak surface anchoring.

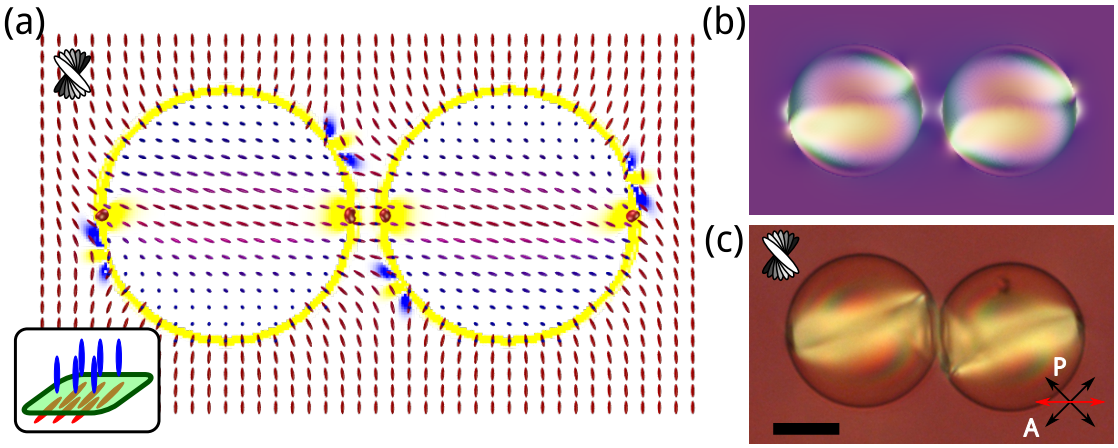

Figure 4. Droplet dimer simulations and experiments. (**a**) Simulated director for homeotropic outer and planar inner anchoring, with a surface-bound disclination connecting the droplets. (**b**) A simulated and (**c**) experimental transmission micrograph of discotic droplets surrounded by the nematic E18 in a twisted planar cell of thickness 50 µm. The crossed polarizers are directed along the rubbing directions on the top and bottom plate. Mass fraction of the discotic material is 11%. The scale bar corresponds to 10 µm. Photo: Giorgio Mirri, IJS (used with permission).

The best matching with the experimental photos is achieved for the combination, where the outside surface anchoring is of the homeotropic type, discotic inside the droplets anchors planar degenerate on the surface and both directors are aligned perpendicular towards each other. Both nematic-surface anchoring strengths are set to a weaker value than in the previous simulations, at $W_{1S}^{\mathrm{deg}} = W_{2S}^{\mathrm{hom}} = 10^{-4}\,\mathrm{J/m^2}$, while the nematic-nematic coupling remains at $W_{12}^{\mathrm{deg}} = 10^{-3}\,\mathrm{J/m^2}$. With these conditions, the simulated polarization image reproduces a surface-bound defect line. The simulated director field in Figure 4a shows that the inside of the droplet has a bipolar structure,

expected for planar surface anchoring. Due to the overlap of outside and inside textures with unknown optical birefringence of the inner phase, makes the transmission image less clear inside the droplets (compare Figure 4b,c).

4. Conclusions

With the development of different composite materials, understanding and simulations of anisotropic-anisotropic coupling are becoming increasingly relevant. We presented a two-phase numerical model for simulations of such materials, and tested various combinations of coupling between both directors and the surface normal. We showed, that in some cases, the coupling leaves the outer and inner media remain largely independent, while in others, the director structures affect each other. For weakly coupled interior textures, reorientation could be possible with very small external fields or deformations, which is suitable for switching or sensors. This is the most important case for future investigation, as differences in elasticity and chirality between the phases can affect the entire structure. The most promising is surface coupling that ensures both director to be perpendicular to each other, but tangent to the interface. Defects can be shared between the media, and their size and shape can depend on properties of both media and the strength of the interaction at the interface. This offers more control over shape of the disclination and consequently, the interface.

With the ground work laid down, targeted simulations can be done for specific experimental cases. The material parameters and coupling constants can be tuned to each case. In this work, we did not focus much on combinations of the three anchorings that have different strengths, or the cases where one of the anchorings is absent or negligible. This is left for future case-specific investigations. As an example, we included a model experiment with a discotic-calamitic mixture, where we have shown that simulations can capture the essence of the behaviour at the interface. This opens the path for further experimental studies of this system, and other such mixtures, where interactions at the interface can have important effects on the optical properties of the system.

Finally, two-phase models are a common way to simulate full hydrodynamics with free interfaces. Anisotropic director coupling across the surface can be easily applied to such simulations without much effort. This is relevant especially for shape-control via elastic constants, two-phase systems involving an active nematic component, or mixtures in a microfluidic setting.

Author Contributions: S.Č. devised and supervised the research. R.G. performed the simulations and analyzed the data. S.Č. and R.G. wrote the paper. All authors have read and agreed to the published version of the manuscript.

Funding: This work was funded by Javna Agencija za Raziskovalno Dejavnost RS (ARRS), grant numbers P1-0099 and J1-9149.

Acknowledgments: We thank Giorgio Mirri, Gregor Posnjak and Igor Muševič for insightful discussions and for providing an experimental example. S.Č. acknowledges support within the COST Action CA17139.

Conflicts of Interest: The authors declare no conflict of interest.

References

1. Muševič, I. Liquid-crystal micro-photonics. *Liq. Cryst. Rev.* **2016**, *4*, 1–34. [CrossRef]
2. Poulin, P.; Stark, H.; Lubensky, T.C.; Weitz, D.A. Novel Colloidal Interactions in Anisotropic Fluids. *Science* **1997**, *275*, 1770. [CrossRef] [PubMed]
3. Lavrentovich, O.D. Topological defects in dispersed liquid crystals, or words and worlds around liquid crystal drops. *Liq. Cryst.* **1998**, *24*, 117. [CrossRef]
4. Lopez-Leon, T.; Fernandez-Nieves, A. Drops and shells of liquid crystal. *Colloid. Polym. Sci.* **2011**, *289*, 345. [CrossRef]
5. Čopar, S. Topology and geometry of nematic braids. *Phys. Rep.* **2014**, *538*, 1–37. [CrossRef]
6. Guillamat, P.; Ignés-Mullol, J.; Sagués, F. Taming active turbulence with patterned soft interfaces. *Nat. Commun.* **2017**, *8*, 1143. [CrossRef]

7. Guillamat, P.; Kos, Ž.; Hardoüin, J.; Ignés-Mullol, J.; Ravnik, M.; Sagués, F. Active nematic emulsions. *Sci. Adv.* **2018**, *4*, eaao1470. [CrossRef]
8. Williams, R.D. Two transitions in tangentially anchored nematic droplets. *J. Phys. A: Math. Gen.* **1986**, *19*, 3211. [CrossRef]
9. Berggren, E.; Zannoni, C.; Chiccoli, C.; Pasini, P.; Semeria, F. Computer simulations of nematic droplets with bipolar boundary conditions. *Phys. Rev. E* **1994**, *50*, 2929. [CrossRef]
10. Xu, F.; Kitzerow, H.S.; Crooker, P. Director configurations of nematic-liquid-crystal droplets: Negative dielectric anisotropy and parallel surface anchoring. *Phys. Rev. E* **1994**, *49*, 3061. [CrossRef]
11. Volovik, G.; Lavrentovich, O. Topological dynamics of defects: Boojums in nematic drops. *Zhurnal Eksperimental'noi i Teoreticheskoi Fiziki* **1983**, *85*, 1159.
12. Seč, D.; Porenta, T.; Ravnik, M.; Žumer, S. Geometrical frustration of chiral ordering in cholesteric droplets. *Soft Matter* **2012**, *8*, 11982–11988. [CrossRef]
13. Seč, D.; Čopar, S.; Žumer, S. Topological zoo of free-standing knots in confined chiral nematic fluids. *Nat. Commun.* **2014**, *5*, 3057. [CrossRef] [PubMed]
14. Posnjak, G.; Čopar, S.; Muševič, I. Points, skyrmions and torons in chiral nematic droplets. *Sci. Rep.* **2016**, *6*, 26361. [CrossRef]
15. De Gennes, P.G.; Prost, J. *The Physics of Liquid Crystals*; Oxford University Press: Oxford, UK, 1993.
16. Kleman, M.; Laverntovich, O.D. *Soft Matter Physics: An Introduction*; Springer: Berlin/Heidelberg, Germany, 2003.
17. Ravnik, M.; Alexander, G.P.; Yeomans, J.M.; Žumer, S. Mesoscopic modelling of colloids in chiral nematics. *Faraday Discuss.* **2009**, *144*, 159–169. [CrossRef]
18. Ravnik, M.; Žumer, S. Landau–de Gennes modelling of nematic liquid crystal colloids. *Liq. Cryst.* **2009**, *36*, 1201–1214. [CrossRef]
19. Willman, E.; Fernandez, F.; James, R.; Day, S. Modeling of Weak Anisotropic Anchoring of Nematic Liquid Crystals in the Landau–de Gennes Theory. *IEEE Trans. Electron Devices* **2007**, *54*, 2630–2637. [CrossRef]
20. Junseok, K. Phase-Field Models for Multi-Component Fluid Flows. *Commun. Comput. Phys.* **2012**, *12*, 613–661. [CrossRef]
21. Diewald, F.; Kuhn, C.; Blauwhoff, R.; Heier, M.; Becker, S.; Werth, S.; Horsch, M.; Hasse, H.; Müller, R. Simulation of Surface Wetting by Droplets Using a Phase Field Model. *PAMM* **2016**, *16*, 519–520. [CrossRef]
22. Tanaka, H.; Araki, T. Simulation Method of Colloidal Suspensions with Hydrodynamic Interactions: Fluid Particle Dynamics. *Phys. Rev. Lett.* **2000**, *85*, 1338. [CrossRef]
23. Fournier, J.B.; Galatola, P. Modeling planar degenerate wetting and anchoring in nematic liquid crystals. *Europhys. Lett. (EPL)* **2005**, *72*, 403–409. [CrossRef]
24. DeBenedictis, A.; Atherton, T.J. Shape minimisation problems in liquid crystals. *Liq. Cryst.* **2016**, *43*, 2352–2362. [CrossRef]
25. Weirich, K.L.; Dasbiswas, K.; Witten, T.A.; Vaikuntanathan, S.; Gardel, M.L. Self-organizing motors divide active liquid droplets. *Proc. Natl. Acad. Sci. USA* **2019**, *116*, 11125. [CrossRef] [PubMed]
26. Zhang, R.; Zhou, Y.; Martinez-Gonzalez, J.A.; Hernandez-Ortiz, J.P.; Abbott, N.L.; de Pablo, J.J. Controlled deformation of vesicles by flexible structured media. *Sci. Adv.* **2016**, *2*, e1600978. [CrossRef]
27. Stark, H. Director field configurations around a spherical particle in a nematic liquid crystal. *Eur. Phys. J. B* **1999**, *10*, 311. [CrossRef]
28. Mkaddem, S.; Gartland, E. Fine structure of defects in radial nematic droplets. *Phys. Rev. E* **2000**, *62*, 6694. [CrossRef]
29. Porenta, T.; Ravnik, M.; Žumer, S. Effect of flexoelectricity and order electricity on defect cores in nematic droplets. *Soft Matter* **2011**, *7*, 132–136. [CrossRef]
30. Čopar, S.; Porenta, T.; Žumer, S. Visualisation methods for complex nematic fields. *Liq. Cryst.* **2013**, *40*, 1759–1768. [CrossRef]
31. Posnjak, G.; Čopar, S.; Muševič, I. Hidden topological constellations and polyvalent charges in chiral nematic droplets. *Nat. Commun.* **2017**, *8*, 14594. [CrossRef]
32. Čopar, S.; Aplinc, J.; Kos, Ž.; Žumer, S.; Ravnik, M. Topology of Three-Dimensional Active Nematic Turbulence Confined to Droplets. *Phys. Rev. X* **2019**, *9*, 031051.

33. Zhou, Y.; Bukusoglu, E.; Martínez-González, J.A.; Rahimi, M.; Roberts, T.F.; Zhang, R.; Wang, X.; Abbott, N.L.; de Pablo, J.J. Structural Transitions in Cholesteric Liquid Crystal Droplets. *ACS Nano* **2016**, *10*, 6484. [CrossRef]
34. Ravnik, M.; Žumer, S. Nematic colloids entangled by topological defects. *Soft Matter* **2009**, *5*, 269. [CrossRef]
35. Araki, T.; Tanaka, H. Colloidal Aggregation in a Nematic Liquid Crystal: Topological Arrest of Particles by a Single-Stroke Disclination Line. *Phys. Rev. Lett.* **2006**, *97*, 127801. [CrossRef] [PubMed]
36. Alexander, G.; Chen, B.; Matsumoto, E.; Kamien, R.D. Colloquium: Disclination loops, point defects, and all that in nematic liquid crystals. *Rev. Mod. Phys.* **2012**, *84*, 497–514. [CrossRef]
37. Kumar, S.; Varshney, S.K.; Chauhan, D. Room-Temperature Discotic Nematic Liquid Crystals. *Mol. Cryst. Liq. Cryst.* **2003**, *396*, 241. [CrossRef]
38. Ravnik, M.; Škarabot, M.; Žumer, S.; Tkalec, U.; Poberaj, I.; Babič, D.; Osterman, N.; Muševič, I. Entangled Nematic Colloidal Dimers and Wires. *Phys. Rev. Lett.* **2008**, *99*, 247801. [CrossRef]